JACS
JOURNAL OF THE AMERICAN CHEMICAL SOCIETY
pubs.acs.org/JACS
Communication

Identifying Poly(ADP-ribose)-Binding Proteins with Photoaffinity-Based Proteomics

Morgan Dasovich, Morgan Q. Beckett, Scott Bailey, Shao-En Ong, Marc M. Greenberg,* and Anthony K. L. Leung*

Cite This: J. Am. Chem. Soc. 2021, 143, 3037−3042
Read Online
ACCESS | Metrics & More | Article Recommendations | Supporting Information

ABSTRACT: Post-translational modification of proteins with poly(ADP-ribose) (PAR) is an important component of the DNA damage response. Four PAR synthesis inhibitors have recently been approved for the treatment of breast, ovarian, and prostate cancers. Despite the clinical significance of PAR, a molecular understanding of its function, including its binding partners, remains incomplete. In this work, we synthesized a PAR photoaffinity probe that captures and isolates endogenous PAR binders. Our method identified dozens of known PAR-binding proteins and hundreds of novel candidates involved in DNA repair, RNA processing, and metabolism. PAR binding by eight candidates was confirmed using pull-down and/or electrophoretic mobility shift assays. Using PAR probes of defined lengths, we detected proteins that preferentially bind to 40-mer versus 8-mer PAR, indicating that polymer length may regulate the outcome and timing of PAR signaling pathways. This investigation produces the first census of PAR-binding proteins, provides a proteomics analysis of length-selective PAR binding, and associates PAR binding with RNA metabolism and the formation of biomolecular condensates.

Poly(ADP-ribose) (PAR) is an NAD^+-dependent post-translational modification (PARylation) synthesized by PAR polymerases (PARPs).[1−6] PARP inhibitors, which have garnered four FDA approvals in the past 6 years, are used to treat cancers.[7] Preclinical data also support repurposing these anticancer drugs as therapeutics for neurodegeneration, cardiac failure, and inflammation.[8] A major function of PARylation is the recruitment of proteins through non-covalent interactions. For instance, PARP1 synthesizes PAR within seconds following DNA strand scission.[9] These PAR chains in turn recruit DNA repair proteins to the damaged sites, locally concentrating repair processes precisely where and when they are needed on the chromatin.[10] Understanding of PAR-dependent processes has been bolstered by proteomics methods that have identified thousands of ADP-ribosylated proteins during genotoxic stress and other contexts.[10−16] However, complementary proteomics methods that identify non-covalent PAR interactions are currently lacking. Here, we describe a photo-cross-linking-based approach that identifies PAR-binding proteins.

Antibody-based approaches have been used to characterize the PAR interactome, which includes PAR binders, PARylated proteins, and indirect interactors, making it difficult to identify direct PAR−protein interactions.[17,18] To date, 92 proteins have been shown to bind PAR directly (Table S1).[19,20] This number is relatively small compared to RNA- and DNA-binding proteins (1541 and 2765, respectively).[21,22] Therefore, we reasoned that many PAR-binding proteins remain undiscovered. A census of the PAR-binding proteome would provide greater insight into PAR-dependent pathways such as DNA repair and may reveal novel biology.

Photo-cross-linking strategies have been used widely to identify proteins that bind to RNA.[23,24] Cross-linking is advantageous since it covalently traps binders, allowing for stringent washes that remove indirect interactions. Since PAR and RNA are structurally similar, we envisioned employing a cross-linking strategy to identify PAR-binding proteins. We synthesized a photoaffinity probe (PARprolink, Figure 1a) consisting of: PAR of defined length, a biotin handle for enrichment, and a single, randomly incorporated photo-inducible cross-linker to stabilize PAR−protein interactions. PARs of defined length were purified from an *in vitro* enzymatic reaction using anion exchange chromatography.[25] The biotin handle was incorporated at the 2′-OH-terminus of PAR using the ELTA bioconjugation technique.[26] We took advantage of the selective modification of RNA hydroxyl groups by activated carboxylic acids to randomly incorporate the benzophenone tethered photo-inducible cross-linker on PAR via a nicotinic acid imidazolide.[27−29] Polymers containing a single benzophenone modification were purified from a PAR mixture composed mostly of 0, 1, and 2 conjugated nicotinic acid analogues by C_{18} reverse-phase HPLC (Figures 1b and S1).

The specificity of PARprolink for PAR-binding proteins was examined by incubating the probe with an increasing amount of either the PAR-binding WWE domain from human RNF146 or bovine serum albumin (BSA). Mixtures were then irradiated (350 nm, 10 min), separated by SDS-PAGE, and transferred to

Received: November 23, 2020
Published: February 17, 2021

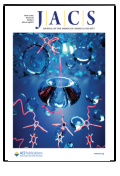

https://dx.doi.org/10.1021/jacs.0c12246
J. Am. Chem. Soc. 2021, 143, 3037−3042

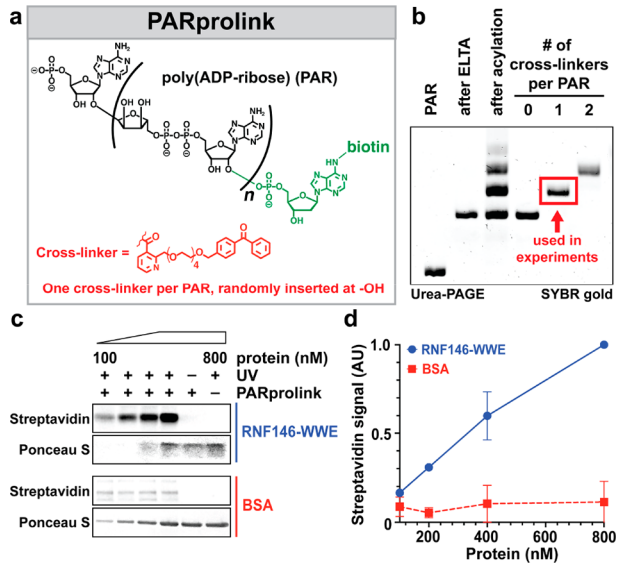

Figure 1. PARprolink selectively captures PAR-binding proteins *in vitro*. (a) PARprolink structure, where each PAR molecule contains one randomly incorporated benzophenone cross-linker. (b) PAGE analyses of PARprolink at each synthetic step. (c) PARprolink (100 nM) was mixed with the indicated concentrations of protein and irradiated at 350 nm, and PAR–protein cross-link formation was detected with streptavidin. (d) Quantification of streptavidin signal from (c); values represent mean ± s.d. (n = 3).

nitrocellulose, which selectively retains protein but not PAR.[30] Irradiation of PARprolink incubated with WWE, but not BSA, formed a protein cross-link that could be detected with streptavidin in a dose-dependent manner (Figures 1c,d and S2a). This signal was dependent on UV irradiation and the presence of PARprolink, consistent with covalent conjugation of the PAR-binding domain to the biotinylated probe. PARprolink specificity was further demonstrated in a complex background by cross-linking WWE domain dosed in cell extracts (Figure S2b). Addition of unlabeled PAR reduced the streptavidin signal on WWE (Figure S2c), suggesting that cross-link formation depends on the PAR–WWE interaction.

Given that most characterized PAR-dependent processes occur in the nucleus, we tested whether our probe can identify endogenous PAR binders in nuclear extracts. We irradiated HeLa nuclear extract incubated with either an 8-mer PARprolink or biotinylated 8-mer PAR lacking benzophenone (negative control) in the presence of an inhibitor against PAR glycohydrolase. PAR–protein cross-links were isolated with streptavidin, then subjected to on-bead trypsin digestion (Figures 2a and S3a and Table S1). LC-MS/MS analysis of the pull-downs identified 798 proteins with two unique peptides in two replicates, and their abundance was quantified using the label-free quantification technology MaxLFQ (Figure S3b).[31] The majority (743, 93%) were at least 2-fold more abundant in the pull-down with PARprolink than in the no-cross-linker control (Figure 2b), demonstrating that the stringent wash removed most non-covalent interactions. There was no correlation between LFQ intensity and protein copy number, further indicating a specific enrichment by PARprolink (Figure S3c). The identified proteins overlap significantly with those identified by two antibody-based PAR interactome studies (P = 6.05 × 10^{-111} and 1.10 × 10^{-103}; Figure S3d and Table S1).[17,18] Although PARprolink identified a similar number of overall proteins as either antibody-based approach, our cross-linking approach captured a greater percentage of known PAR binders (39 out of 92 (42%); Figure S3e and Table S1).[19,20]

To further validate that PARprolink identifies direct PAR–protein interactions, we expressed and purified eight candidates (AK2, CAPRIN1, DDX6, G3BP2, UHRF1, G3BP1, GAPDH, and PARP1) and subjected them to two PAR-binding assays. Initially, the candidate proteins were incubated with a mixture of biotinylated PAR of different lengths, followed by streptavidin pull-down. The specificity of the assay was validated with the WWE domain and BSA as a negative control.

We confirmed a direct interaction between PAR and seven out of eight candidates (Figures 2c and S4). The affinities of these candidates for 16-mer PAR were determined by electromobility shift assays (EMSAs) (Table 1 and Figure S5). Consistent with our qualitative pull-down assay, the same seven candidates had affinities for PAR within the range

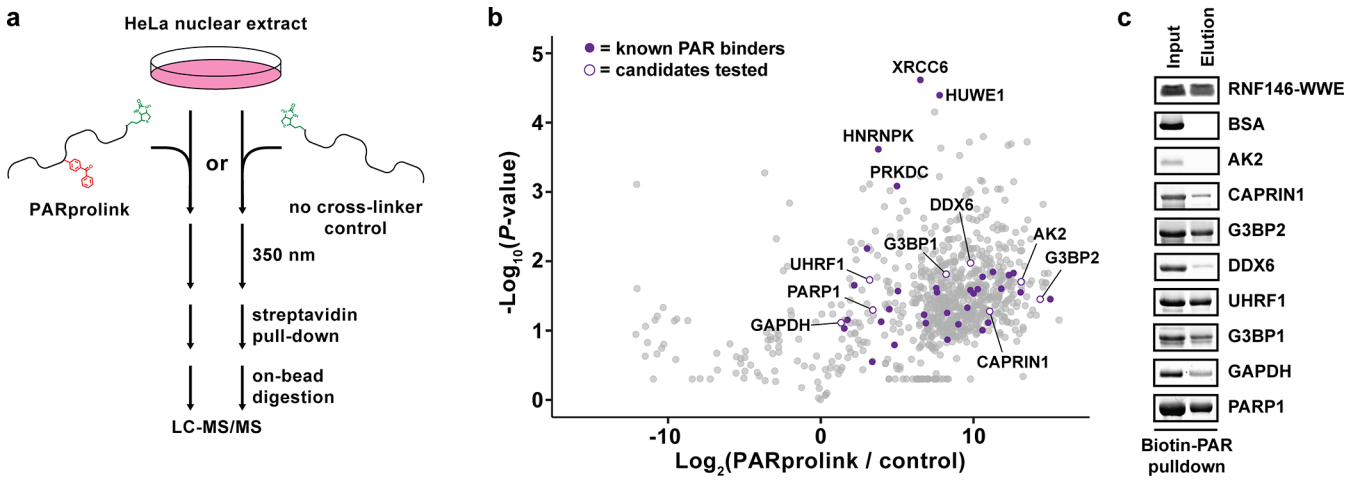

Figure 2. Photoaffinity-based isolation of the endogenous PAR-binding proteome. (a) Proteomics workflow schematic. (b) Volcano plot of protein Log_2 enrichment ratios and $-Log_{10}$(P-values) from proteomics experiments (n = 2). (c) Non-covalent biotin-PAR pull-downs with recombinantly expressed PAR-binding candidates.

https://dx.doi.org/10.1021/jacs.0c12246
J. Am. Chem. Soc. 2021, 143, 3037–3042

Table 1. Summary of PAR−Protein Affinities Measured with EMSAs

protein	K_D (nM)	95% CI (nM)	R^2
AK2	~46 000	33 000−65 000	0.88
CAPRIN1	~3 400	1 500−7 700	0.82
G3BP2	~313	197−497	0.91
DDX6	~199	134−291	0.94
UHRF1	~162	115−230	0.92
G3BP1	~93	73−124	0.95
GAPDH	~54	37−79	0.94
PARP1	~27	20−38	0.93

reported for other PAR-binding proteins (K_D = 1 nM−10 μM).[20,32] The dissociation constant for AK2, which was not detected in the pull-down experiment, was estimated to be 33−65 μM, suggesting the AK2−PAR interaction may not be physiologically relevant. Taken together, these results indicate that PARprolink captured a substantial fraction of the known PAR-binding proteome and enabled the discovery of novel PAR binders.

Having validated that PARprolink identifies PAR-binding proteins, we systematically investigated how endogenous proteins bind to different lengths of PAR. Emergent data suggest that signaling pathways are only activated when PAR length exceeds a certain threshold. Parthanatos, a PAR-dependent cell death pathway, is induced more strongly by long PAR (~60-mer) than short PAR (~15-mer).[33] In addition, three DNA repair-related proteins (XPA, DEK, p53) preferentially bind long PAR, and the Chk1 kinase is only activated by long PAR.[34−36] HeLa nuclear extract was cross-linked to either 8-mer or ~40-mer PAR photoaffinity probes, with a bead-only pull-down as a negative control. Comparing the intensities between these pull-downs uncovered 156 proteins that prefer ~40-mer PAR (Log_2 fold change >2; Figures 3a and S6a and Table S1). Importantly, we observed the long PAR-binding preference of DEK,[34] validating that our approach identifies length-selective PAR binders.

Intriguingly, our analyses revealed that the central DNA repair protein PARP1 preferred binding to long PAR (~40-mer/8-mer = 13, Figure 3a). To verify this finding, EMSAs were performed with recombinant PARP1 and PAR of varied lengths (Figures 3b and S6b,c). We observed a 16-fold increase in PARP1−PAR affinity as PAR length increased from 4- to 16-mer. Importantly, the affinity of the PARP1−PAR interactions for the 16- and 32-mers (K_D = 11−110 nM) is in the same range as the reported affinities between PARP1 and nucleosomes (K_D = 2−100 nM).[37] These PARP1−PAR interactions can be disrupted by PARP1 automodification (Figure S6d). Given that PAR length is controlled temporally during DNA damage, where long polymers (>22-mer) are rapidly synthesized by PARP1 and then slowly degraded to shorter lengths,[27,38] our data suggest that PAR length may control the dissociation of PARP1 from the chromatin during DNA repair.

Our investigation represents the first census of PAR binders. We took this opportunity to analyze properties of the identified PAR-binding proteome. Gene ontology (GO) analysis on all 743 PAR-binding candidates (Figure 2b) revealed the expected enrichment of several DNA repair pathways (Figure S7).[17] Yet, the enrichments of physiological processes such as RNA splicing, RNA transport, and DNA replication were even more significant. Notably, long PAR binders are enriched with

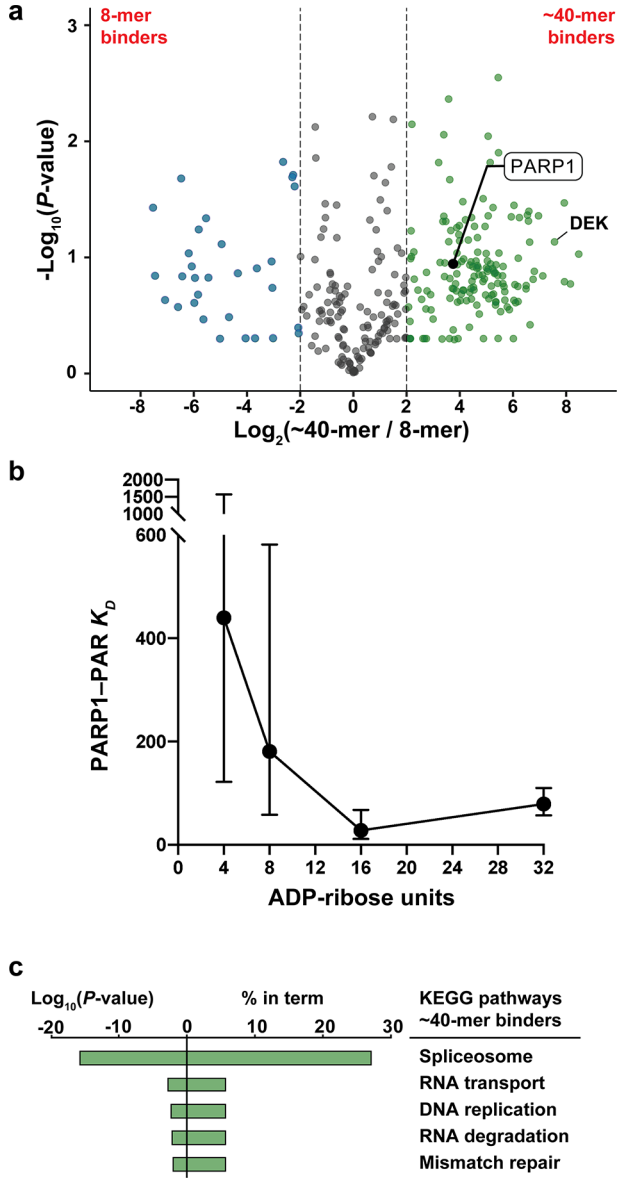

Figure 3. Defined-length probes reveal length-specific PAR−protein interactions. (a) Volcano plot of protein Log_2 enrichment ratios and − Log_{10} *P*-values from proteomics experiments using either 8- or ~40-mer probes (n = 2). (b) The effect of PAR length on the affinity toward PARP1 measured with EMSA (K_D ± 95% CI; n = 3). (c) Gene ontology analysis of proteins that were more abundant in the ~40-mer pull-down (enrichment ratio >4).

proteins involved in nucleic acid metabolism, such as DNA repair and RNA splicing (Figure 3c). STRING protein association network analyses mapped two central cores—one involved in DNA repair and chromatin remodeling, and the other in RNA splicing and translation—along with distal clusters involved in metabolism and tRNA synthesis (Figures 4a and S8). Consistent with recent proteomics studies identifying ADP-ribosylated substrates,[10−16] our analysis of PAR-binding candidates strengthens the view that PAR has roles beyond DNA repair in metabolism and RNA regulation.[39,40]

We next assessed the enrichment of protein domains from the Pfam database in our dataset (Figures 4b and S9a,b and Table S1).[41−43] We observed a significant enrichment of multiple helicase-associated domains among PAR-binding

https://dx.doi.org/10.1021/jacs.0c12246
J. Am. Chem. Soc. 2021, 143, 3037−3042

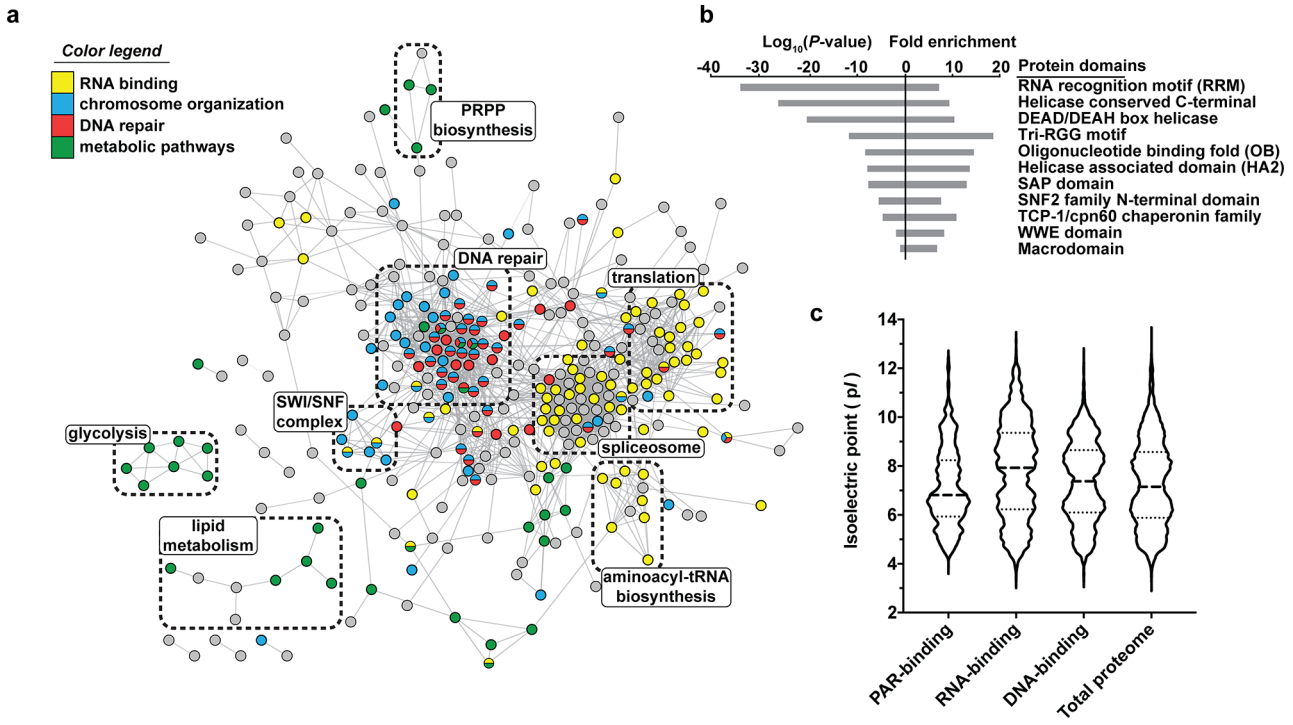

Figure 4. Analyses of the PAR-binding proteome. (a) STRING network analysis of high-confidence PAR-binding candidates (enrichment ratio >8, $P < 0.05$, 416 genes) displaying at least one connection to another candidate. (b) Enrichment of known PAR-binding and other domains. (c) p*I* distribution among PAR-, RNA-, and DNA-binding proteins.

candidates. Consistently, helicase activity is the most enriched molecular function based on GO analyses (Figure S7). Several known PAR-binding domains, such as WWE domain and macrodomain, were also enriched. Among them, the most significant was the Tri-RGG motif, with 12 out of 16 Tri-RGG-containing proteins in the human proteome identified. In addition, we observed the enrichment of DNA/RNA-binding domains known to bind PAR, e.g., the RNA recognition motif and OB-fold.[44] Therefore, it is not surprising that a significant amount of PAR-binding candidates are also known DNA- or RNA-binding proteins($P = 3.57 \times 10^{-6}$ and 2.00×10^{-136}; Table S1).[21,22] RNA- and DNA-binding proteins tend to have higher isoelectric points (median pI = 7.93 and 7.38). Unexpectedly, the median isoelectric point of PAR-binding candidates was lower than the proteome (pI = 6.81 vs 7.15, Figures 4c and S9c–f). Together, these data suggest a specific interaction between PAR and particular protein domains, rather than a non-specific enrichment of positively charged proteins.

In addition to defined motifs or domains, PAR-binding candidates were statistically enriched with proteins containing low-complexity sequence ($P \leq 5.5 \times 10^{-18}$),[45,46] which is critical for the formation of biomolecular condensates.[47] Indeed, PARprolink identified proteins enriched with components of biomolecular condensates such as DNA repair foci, nucleoli, and stress granules ($P = 8.36 \times 10^{-21}$, 2.34×10^{-57}, and 5.97×10^{-94}; Table S1).[48−50] Notably, PARylation of the DNA repair factor p53 and the nucleolar helicase DDX21 is dependent on their ability to bind PAR.[51,52] Consistent with these studies, comparison with proteomics analyses of ADP-ribosylated substrates revealed that most PAR-binding candidates are also ADP-ribosylated (647 out of 743 (87%), $P = 1.43 \times 10^{-246}$; Table S1).[53] Taken together, our data suggest that one or more PARylation events may trigger a wave of PAR binding-dependent PARylation in their vicinity, building extensive PAR−protein interaction networks to form biomolecular condensates in cells.[6,54]

This work describes the first proteomics method developed to identify direct PAR binders. Our census sheds lights into PAR−protein interactions involved in DNA repair, RNA regulation, and biomolecular condensate formation, thereby serving as a rich resource to explore these frontiers in PAR biology.

■ ASSOCIATED CONTENT

Supporting Information

The Supporting Information is available free of charge at https://pubs.acs.org/doi/10.1021/jacs.0c12246.

Experimental methods, Figures S1−S9, and NMR spectra of new compounds (PDF)

Table S1, proteomics data and analysis (XLSX)

■ AUTHOR INFORMATION

Corresponding Authors

Marc M. Greenberg − *Department of Chemistry, Krieger School of Arts and Sciences, Johns Hopkins University, Baltimore, Maryland 21218, United States;* orcid.org/0000-0002-5786-6118; Email: mgreenberg@jhu.edu

Anthony K. L. Leung − *Department of Biochemistry and Molecular Biology, Bloomberg School of Public Health, Department of Molecular Biology and Genetics, School of Medicine, and Department of Oncology, School of Medicine, Johns Hopkins University, Baltimore, Maryland 21205, United States;* orcid.org/0000-0001-5569-4036; Email: anthony.leung@jhu.edu

https://dx.doi.org/10.1021/jacs.0c12246
J. Am. Chem. Soc. 2021, 143, 3037−3042

Authors

Morgan Dasovich − *Department of Chemistry, Krieger School of Arts and Sciences and Department of Biochemistry and Molecular Biology, Bloomberg School of Public Health, Johns Hopkins University, Baltimore, Maryland 21218, United States*

Morgan Q. Beckett − *Department of Biophysics and Biophysical Chemistry, School of Medicine, Johns Hopkins University, Baltimore, Maryland 21205, United States*

Scott Bailey − *Department of Biophysics and Biophysical Chemistry, School of Medicine and Department of Biochemistry and Molecular Biology, Bloomberg School of Public Health, Johns Hopkins University, Baltimore, Maryland 21205, United States*

Shao-En Ong − *Department of Pharmacology, University of Washington, Seattle, Washington 98195, United States;* orcid.org/0000-0003-3314-5903

Complete contact information is available at: https://pubs.acs.org/10.1021/jacs.0c12246

Notes

The authors declare no competing financial interest.

■ ACKNOWLEDGMENTS

We thank Dr. Srinivasan Yegnasubramanian for the UHRF1 plasmid; Dr. J. Paul Taylor for G3BP1 protein and plasmids for G3BP2, DDX6, and CAPRIN1; Dr. John Pascal for the PARP1 plasmid; and Tim Mitchison for *in vitro* synthesized PAR. We would like to thank Robert O'Meally, Tatiana Boronina (Johns Hopkins), and Mark Hail (Novatia) for assistance with the mass analysis. We thank Biorender for providing some artwork used in the TOC graphic. We thank the Johns Hopkins Discovery Award as well as NIH grants T32GM080189, T32GM008403, R01GM104135 (AKLL), R35GM131736 (MMG), and RF1AG071326 (AKLL) for funding.

■ ABBREVIATIONS

RNF146, ring finger protein 146; BSA, bovine serum albumin; AK2, adenylate kinase 2; OB, oligonucleotide/oligosaccharide-binding

■ REFERENCES

(1) Gibson, B. A.; Kraus, W. L. New Insights into the Molecular and Cellular Functions of poly(ADP-Ribose) and PARPs. *Nat. Rev. Mol. Cell Biol.* **2012**, *13* (7), 411−424.

(2) Lüscher, B.; Bütepage, M.; Eckei, L.; Krieg, S.; Verheugd, P.; Shilton, B. H. ADP-Ribosylation, a Multifaceted Posttranslational Modification Involved in the Control of Cell Physiology in Health and Disease. *Chem. Rev.* **2018**, *118* (3), 1092−1136.

(3) Suskiewicz, M. J.; Palazzo, L.; Hughes, R.; Ahel, I. Progress and Outlook in Studying the Substrate Specificities of PARPs and Related Enzymes. *FEBS J.* **2020**, DOI: 10.1111/febs.15518.

(4) Sanderson, D. J.; Cohen, M. S. Mechanisms Governing PARP Expression, Localization, and Activity in Cells. *Crit. Rev. Biochem. Mol. Biol.* **2020**, *55*, 541−554.

(5) Hottiger, M. O. SnapShot: ADP-Ribosylation Signaling. *Mol. Cell* **2015**, *58* (6), 1134−1134.

(6) Leung, A. K. L. Poly(ADP-Ribose): A Dynamic Trigger for Biomolecular Condensate Formation. *Trends Cell Biol.* **2020**, *30* (5), 370−383.

(7) Lord, C. J.; Ashworth, A. PARP Inhibitors: Synthetic Lethality in the Clinic. *Science* **2017**, *355* (6330), 1152−1158.

(8) Berger, N. A.; Besson, V. C.; Boulares, A. H.; Bürkle, A.; Chiarugi, A.; Clark, R. S.; Curtin, N. J.; Cuzzocrea, S.; Dawson, T. M.; Dawson, V. L.; Haskó, G.; Liaudet, L.; Moroni, F.; Pacher, P.; Radermacher, P.; Salzman, A. L.; Snyder, S. H.; Soriano, F. G.; Strosznajder, R. P.; Sümegi, B.; Swanson, R. A.; Szabó, C. Opportunities for the Repurposing of PARP Inhibitors for the Therapy of Non-Oncological Diseases. *Br. J. Pharmacol.* **2018**, *175* (2), 192−222.

(9) Eustermann, S.; Wu, W.-F.; Langelier, M.-F.; Yang, J.-C.; Easton, L. E.; Riccio, A. A.; Pascal, J. M.; Neuhaus, D. Structural Basis of Detection and Signaling of DNA Single-Strand Breaks by Human PARP-1. *Mol. Cell* **2015**, *60* (5), 742−754.

(10) Zhen, Y.; Yu, Y. Proteomic Analysis of the Downstream Signaling Network of PARP1. *Biochemistry* **2018**, *57* (4), 429−440.

(11) Daniels, C. M.; Ong, S.-E.; Leung, A. K. L. The Promise of Proteomics for the Study of ADP-Ribosylation. *Mol. Cell* **2015**, *58* (6), 911−924.

(12) Buch-Larsen, S. C.; Hendriks, I. A.; Lodge, J. M.; Rykær, M.; Furtwängler, B.; Shishkova, E.; Westphall, M. S.; Coon, J. J.; Nielsen, M. L. Mapping Physiological ADP-Ribosylation Using Activated Ion Electron Transfer Dissociation. *Cell Rep.* **2020**, *32* (12), 108176.

(13) Nowak, K.; Rosenthal, F.; Karlberg, T.; Bütepage, M.; Thorsell, A.-G.; Dreier, B.; Grossmann, J.; Sobek, J.; Imhof, R.; Lüscher, B.; Schüler, H.; Plückthun, A.; Leslie Pedrioli, D. M.; Hottiger, M. O. Engineering Af1521 Improves ADP-Ribose Binding and Identification of ADP-Ribosylated Proteins. *Nat. Commun.* **2020**, *11* (1), 5199.

(14) Carter-O'Connell, I.; Jin, H.; Morgan, R. K.; David, L. L.; Cohen, M. S. Engineering the Substrate Specificity of ADP-ribosyltransferases for Identifying Direct Protein Targets. *J. Am. Chem. Soc.* **2014**, *136* (14), 5201−5204.

(15) Jiang, H.; Kim, J. H.; Frizzell, K. M.; Kraus, W. L.; Lin, H. Clickable NAD Analogues for Labeling Substrate Proteins of Poly(ADP-ribose) Polymerases. *J. Am. Chem. Soc.* **2010**, *132* (27), 9363−9372.

(16) Gibson, B. A.; Zhang, Y.; Jiang, H.; Hussey, K.; Shrimp, J. H.; Lin, H.; Schwede, F.; Yu, Y.; Kraus, W. L Chemical genetic discovery of PARP targets reveals a role for PARP-1 in transcription elongation. *Science* **2016**, *353* (6294), 45−50.

(17) Gagné, J.-P.; Pic, E.; Isabelle, M.; Krietsch, J.; Ethier, C.; Paquet, E.; Kelly, I.; Boutin, M.; Moon, K.-M.; Foster, L. J.; Poirier, G. G. Quantitative Proteomics Profiling of the poly(ADP-Ribose)-Related Response to Genotoxic Stress. *Nucleic Acids Res.* **2012**, *40* (16), 7788−7805.

(18) Wright, R. H. G.; Lioutas, A.; Le Dily, F.; Soronellas, D.; Pohl, A.; Bonet, J.; Nacht, A. S.; Samino, S.; Font-Mateu, J.; Vicent, G. P.; Wierer, M.; Trabado, M. A.; Schelhorn, C.; Carolis, C.; Macias, M. J.; Yanes, O.; Oliva, B.; Beato, M. ADP-Ribose-Derived Nuclear ATP Synthesis by NUDIX5 Is Required for Chromatin Remodeling. *Science* **2016**, *352* (6290), 1221−1225.

(19) Teloni, F.; Altmeyer, M. Readers of poly(ADP-Ribose): Designed to Be Fit for Purpose. *Nucleic Acids Res.* **2016**, *44* (3), 993−1006.

(20) Krietsch, J.; Rouleau, M.; Pic, É.; Ethier, C.; Dawson, T. M.; Dawson, V. L.; Masson, J.-Y.; Poirier, G. G.; Gagné, J.-P. Reprogramming Cellular Events by poly(ADP-Ribose)-Binding Proteins. *Mol. Aspects Med.* **2013**, *34* (6), 1066−1087.

(21) Gerstberger, S.; Hafner, M.; Tuschl, T. A Census of Human RNA-Binding Proteins. *Nat. Rev. Genet.* **2014**, *15* (12), 829−845.

(22) Lambert, S. A.; Jolma, A.; Campitelli, L. F.; Das, P. K.; Yin, Y.; Albu, M.; Chen, X.; Taipale, J.; Hughes, T. R.; Weirauch, M. T. The Human Transcription Factors. *Cell* **2018**, *175* (2), 598−599.

(23) Castello, A.; Fischer, B.; Eichelbaum, K.; Horos, R.; Beckmann, B. M.; Strein, C.; Davey, N. E.; Humphreys, D. T.; Preiss, T.; Steinmetz, L. M.; Krijgsveld, J.; Hentze, M. W. Insights into RNA Biology from an Atlas of Mammalian mRNA-Binding Proteins. *Cell* **2012**, *149* (6), 1393−1406.

(24) Arguello, A. E.; DeLiberto, A. N.; Kleiner, R. E. RNA Chemical Proteomics Reveals the N6-Methyladenosine (m6A)-Regulated Protein-RNA Interactome. *J. Am. Chem. Soc.* **2017**, *139* (48), 17249−17252.

(25) Tan, E. S.; Krukenberg, K. A.; Mitchison, T. J. Large Scale Preparation and Characterization of poly(ADP-Ribose) and Defined Length Polymers. *Anal. Biochem.* **2012**, *428* (2), 126−136.
(26) Ando, Y.; Elkayam, E.; McPherson, R. L.; Dasovich, M.; Cheng, S.-J.; Voorneveld, J.; Filippov, D. V.; Ong, S.-E.; Joshua-Tor, L.; Leung, A. K. L. ELTA: Enzymatic Labeling of Terminal ADP-Ribose. *Mol. Cell* **2019**, *73* (4), 845−856.
(27) Spitale, R. C.; Crisalli, P.; Flynn, R. A.; Torre, E. A.; Kool, E. T.; Chang, H. Y. RNA SHAPE Analysis in Living Cells. *Nat. Chem. Biol.* **2013**, *9* (1), 18−20.
(28) Mortimer, S. A.; Weeks, K. M. Time-resolved RNA SHAPE Chemistry. *J. Am. Chem. Soc.* **2008**, *130* (48), 16178−16180.
(29) Dormán, G.; Prestwich, G. D. Benzophenone photophores in Biochemistry. *Biochemistry* **1994**, *33* (19), 5661−5673.
(30) Wong, I.; Lohman, T. M. A Double-Filter Method for Nitrocellulose-Filter Binding: Application to Protein-Nucleic Acid Interactions. *Proc. Natl. Acad. Sci. U. S. A.* **1993**, *90* (12), 5428−5432.
(31) Cox, J.; Hein, M. Y.; Luber, C. A.; Paron, I.; Nagaraj, N.; Mann, M. Accurate Proteome-Wide Label-Free Quantification by Delayed Normalization and Maximal Peptide Ratio Extraction, Termed MaxLFQ. *Mol. Cell. Proteomics* **2014**, *13* (9), 2513−2526.
(32) Li, M.; Lu, L.-Y.; Yang, C.-Y.; Wang, S.; Yu, X. The FHA and BRCT Domains Recognize ADP-Ribosylation during DNA Damage Response. *Genes Dev.* **2013**, *27* (16), 1752−1768.
(33) Andrabi, S. A.; Kim, N. S.; Yu, S.-W.; Wang, H.; Koh, D. W.; Sasaki, M.; Klaus, J. A.; Otsuka, T.; Zhang, Z.; Koehler, R. C.; Hurn, P. D.; Poirier, G. G.; Dawson, V. L.; Dawson, T. M. Poly(ADP-Ribose) (PAR) Polymer Is a Death Signal. *Proc. Natl. Acad. Sci. U. S. A.* **2006**, *103* (48), 18308−18313.
(34) Fahrer, J.; Kranaster, R.; Altmeyer, M.; Marx, A.; Bürkle, A. Quantitative Analysis of the Binding Affinity of poly(ADP-Ribose) to Specific Binding Proteins as a Function of Chain Length. *Nucleic Acids Res.* **2007**, *35* (21), No. e143.
(35) Fahrer, J.; Popp, O.; Malanga, M.; Beneke, S.; Markovitz, D. M.; Ferrando-May, E.; Bürkle, A.; Kappes, F. High-Affinity Interaction of poly(ADP-Ribose) and the Human DEK Oncoprotein Depends upon Chain Length. *Biochemistry* **2010**, *49* (33), 7119−7130.
(36) Min, A.; Im, S.-A.; Yoon, Y.-K.; Song, S.-H.; Nam, H.-J.; Hur, H.-S.; Kim, H.-P.; Lee, K.-H.; Han, S.-W.; Oh, D.-Y.; Kim, T.-Y.; O'Connor, M. J.; Kim, W.-H.; Bang, Y.-J. RAD51C-Deficient Cancer Cells Are Highly Sensitive to the PARP Inhibitor Olaparib. *Mol. Cancer Ther.* **2013**, *12* (6), 865−877.
(37) Wielckens, K.; Schmidt, A.; George, E.; Bredehorst, R.; Hilz, H. DNA Fragmentation and NAD Depletion. Their Relation to the Turnover of Endogenous mono(ADP-Ribosyl) and poly(ADP-Ribosyl) Proteins. *J. Biol. Chem.* **1982**, *257* (21), 12872−12877.
(38) Muthurajan, U. M.; Hepler, M. R. D.; Hieb, A. R.; Clark, N. J.; Kramer, M.; Yao, T.; Luger, K. Automodification Switches PARP-1 Function from Chromatin Architectural Protein to Histone Chaperone. *Proc. Natl. Acad. Sci. U. S. A.* **2014**, *111* (35), 12752−12757.
(39) Kim, D.-S.; Challa, S.; Jones, A.; Kraus, W. L. PARPs and ADP-Ribosylation in RNA Biology: From RNA Expression and Processing to Protein Translation and Proteostasis. *Genes Dev.* **2020**, *34* (5−6), 302−320.
(40) Szántó, M.; Bai, P. The Role of ADP-Ribose Metabolism in Metabolic Regulation, Adipose Tissue Differentiation, and Metabolism. *Genes Dev.* **2020**, *34* (5−6), 321−340.
(41) Altmeyer, M.; Neelsen, K. J.; Teloni, F.; Pozdnyakova, I.; Pellegrino, S.; Grøfte, M.; Rask, M.-B. D.; Streicher, W.; Jungmichel, S.; Nielsen, M. L.; Lukas, J. Liquid Demixing of Intrinsically Disordered Proteins Is Seeded by poly(ADP-Ribose). *Nat. Commun.* **2015**, *6*, 8088.
(42) Gupte, R.; Liu, Z.; Kraus, W. L. PARPs and ADP-Ribosylation: Recent Advances Linking Molecular Functions to Biological Outcomes. *Genes Dev.* **2017**, *31* (2), 101−126.
(43) Finn, R. D.; Tate, J.; Mistry, J.; Coggill, P. C.; Sammut, S. J.; Hotz, H.-R.; Ceric, G.; Forslund, K.; Eddy, S. R.; Sonnhammer, E. L. L.; Bateman, A. The Pfam Protein Families Database. *Nucleic Acids Res.* **2007**, *36* (Database issue), D281−D288.
(44) Zhang, F.; Chen, Y.; Li, M.; Yu, X. The Oligonucleotide/oligosaccharide-Binding Fold Motif Is a poly(ADP-Ribose)-Binding Domain That Mediates DNA Damage Response. *Proc. Natl. Acad. Sci. U. S. A.* **2014**, *111* (20), 7278−7283.
(45) March, Z. M.; King, O. D.; Shorter, J. Prion-like Domains as Epigenetic Regulators, Scaffolds for Subcellular Organization, and Drivers of Neurodegenerative Disease. *Brain Res.* **2016**, *1647*, 9−18.
(46) Han, T. W.; Kato, M.; Xie, S.; Wu, L. C.; Mirzaei, H.; Pei, J.; Chen, M.; Xie, Y.; Allen, J.; Xiao, G.; McKnight, S. L. Cell-free Formation of RNA Granules: Bound RNAs Identifiy Features and Components of Cellular Assemblies. *Cell* **2012**, *149* (4), 768−779.
(47) Banani, S. F.; Lee, H. O.; Hyman, A. A.; Rosen, M. K. Biomolecular Condensates: Organizers of Cellular Biochemistry. *Nat. Rev. Mol. Cell Biol.* **2017**, *18* (5), 285−298.
(48) Chou, D. M.; Adamson, B.; Dephoure, N. E.; Tan, X.; Nottke, A. C.; Hurov, K. E.; Gygi, S. P.; Colaiácovo, M. P.; Elledge, S. J. A Chromatin Localization Screen Reveals Poly(ADP-ribose)-regulated Recruitment Polycomb and NuRD Complexes to Sites of DNA Damage. *Proc. Natl. Acad. Sci. U. S. A.* **2010**, *107* (43), 18475−18480.
(49) Ahmad, Y.; Boisvert, F.; Gregor, P.; Cobley, A.; Lamond, A. I. NOPdb: Nucleolar Proteome Database—2008 Update. *Nucleic Acids Res.* **2009**, *37* (D1), D181−D184.
(50) Nunes, C.; Mestre, I.; Marcelo, A.; Koppenol, R.; Matos, C. A.; Nóbrega, C. MSGP: the first database of the protein components of the mammalian stress granules. *Database* **2019**, *2019*, baz031.
(51) Fischbach, A.; Krüger, A.; Hampp, S.; Assmann, G.; Rank, L.; Hufnagel, M.; Stöckl, M. T.; Fischer, J. M. F.; Veith, S.; Rossatti, P.; Ganz, M.; Ferrando-May, E.; Hartwig, A.; Hauser, K.; Wiesmüller, L.; Bürkle, A.; Mangerich, A. The C-Terminal Domain of p53 Orchestrates the Interplay between Non-Covalent and Covalent poly(ADP-Ribosyl)ation of p53 by PARP1. *Nucleic Acids Res.* **2018**, *46* (2), 804−822.
(52) Kim, D.-S.; Camacho, C. V.; Nagari, A.; Malladi, V. S.; Challa, S.; Kraus, W. L. Activation of PARP-1 by snoRNAs Controls Ribosome Biogenesis and Cell Growth via the RNA Helicase DDX21. *Mol. Cell* **2019**, *75* (6), 1270−1285.
(53) Ayyappan, V.; Wat, R.; Barber, C.; Vivelo, C. A.; Gauch, K.; Visanpattanasin, P.; Cook, G.; Sazeides, C.; Leung, A. K. L. ADPriboDB 2.0: an updated database of ADP-ribosylated proteins. *Nucleic Acids Res.* **2021**, *49*, D261−D265.
(54) Dasovich, M.; Leung, A. K. L. A Nucleolar PARtnership Expands PARP Roles in RNA Biology and the Clinical Potential of PARP Inhibitors. *Mol. Cell* **2019**, *75* (6), 1089−1091.

https://dx.doi.org/10.1021/jacs.0c12246
J. Am. Chem. Soc. 2021, 143, 3037−3042